Bulletin of Glaciological Research 24 (2007) *71–78*

Meteorological observations during 2002–2004 in Lunana region, Bhutan Himalayas

Ryohei SUZUKI[1], Koji FUJITA[1], Yutaka AGETA[1], Nozomu NAITO[2], Yoshihiro MATSUDA[1] and KARMA[3]

1 Graduate School of Environmental Studies, Nagoya University, c/o HyARC, Chikusa-ku, Nagoya 464–8601, Japan
2 Department of Global Environment Studies, Hiroshima Institute of Technology, Hiroshima 731–5193, Japan
3 Geological Survey of Bhutan, P.O. Box 173, Thimphu, Bhutan

(Received September 30, 2006; Revised manuscript accepted November 13, 2006)

Abstract

Meteorological observations were carried out in the Lunana region, Bhutan Himalayas, from September 2002 to October 2004. An automatic weather station (Lugge AWS) was installed at 4524 m a.s.l. on the end moraine of Lugge Glacier. In addition, air temperatures, ground temperatures and relative humidity were observed simultaneously around the AWS from late September to early October in 2003 and 2004 to investigate spatial variation of these components. Characteristics of seasonal and diurnal variations of meteorological elements are shown using the data observed by the AWS. Relatively large spatial variability of surface temperature is shown by the data observed at different sites compared to that of air temperature and relative humidity.

1. Introduction

Supraglacial lakes, which expand in the termini of debris-covered glaciers due to the glacier shrinkage, have a possibility of Glacial Lake Outburst Floods (GLOFs) that are caused by the collapse of moraines. Such possibilities in northern Bhutan have been pointed out in previous studies (*e.g.,* Ageta *et al.,* 2000; Richardson and Reynolds, 2000; Iwata *et al.,* 2002; Komori *et al.,* 2004). However, no study has been published on meteorological conditions in northern Bhutan.

Surface temperature as well as atmospheric condition is also basic information on debris-covered glaciers. On a debris-covered glacier, the ice melt rate under a debris layer varies with thickness and thermal properties of the debris (*e.g.,* Fujii, 1977; Nakawo and Rana, 1999; Mattson *et al.,* 1993; Benn and Lehmkuhl, 2000). Generally, the melt rate increases with thickness of debris, having a maximum at several centimeters thickness, and then decreasing towards a thickness at which the melt rate equals the rate for a bare ice surface without debris. The melt rate decreases further with a further increase in thickness. However, the range of such variation also depends on the thermal property of debris, which is not uniform among glaciers. Thus, surface temperature is a key element for mass balance studies through investigation of thickness and thermal properties of debris layers (Nakawo and Young, 1981; 1982).

Meteorological observations were carried out in the Lunana region of Bhutan under the Japan-Bhutan joint research project from 2002 to 2004. The outline of this project and activities has been reported in Yamada *et al.* (2004). Climatic conditions around debris-free glaciers in the Bhutan Himalayas were also investigated under the same project, and the results have been reported in Naito *et al.* (2006). The present paper aims to report the meteorological conditions around debris-covered glaciers in the Lunana region of Bhutan.

2. Locations and methods

An automatic weather station (AWS) was installed at 4524 m a.s.l. on the end moraine of Lugge Glacier in the Lunana region of Bhutan. The AWS started to record 9 meteorological elements on 17 September in 2002 (Yamada *et al.,* 2004). The observed meteorological elements, heights of each sensor and observation periods are shown in Table 1. Air temperature was measured with a natural-draft type radiation shield. A platinum resistance thermometer was used for measuring ground surface temperatures. Sand with a thickness of about 1 cm covered the sensor for insulating solar radiation. Ground surface temperature was recorded at 1-hour intervals, and the other meteorological data were recorded at 30-minute intervals. Locations of each measurement are shown

Table 1. Measurements at Lugge automatic weather station.

Meteorological element	Abbreviation	Height (m)	Period
Air temperature	Ta	2	17 Sep., 2002 - 11 Oct., 2004
Relative humidity	Rh	2	17 Sep., 2002 - 11 Oct., 2004
Wind speed	Ws	2	17 Sep., 2002 - 4 Aug., 2004; 1 - 11 Oct., 2004
Wind direction	Wd	2	17 Sep., 2002 - 4 Aug., 2004; 1 - 11 Oct., 2004
Ground temperature	Ts	0	17 Sep., 2002 - 10 Oct., 2003; 1 - 11 Oct., 2004
Precipitation	P	1	17 Sep., 2002 - 11 Oct., 2004
Net radiation	Rn	2	17 Sep., 2002 - 1 Oct., 2003; 29 Sep. - 11 Oct., 2004
Downward shortwave radiation	Sd	2	17 Sep., 2002 - 11 Oct., 2004
Upward shortwave radiation	Su	2	17 Sep., 2002 - 11 Oct., 2004

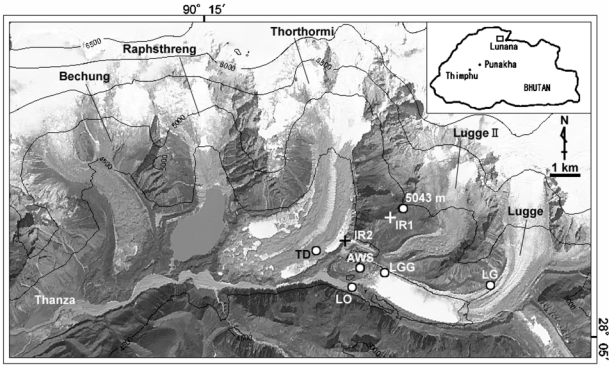

Fig. 1. Locations of meteorological observation sites in a satellite image of Lunana region, Bhutan taken by ASTER band 3N on 20 January, 2001. Contour lines drawn every 500 m are based on ASTER-DEM. The position of Lugge automatic weather station is shown as AWS. Other observation points are also shown in this image using symbols described in Table 2.

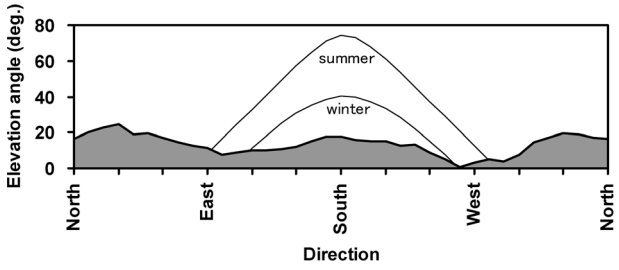

Fig. 2. Elevation angle of mountain skyline at Lugge AWS obtained from digital elevation model of ASTER products. Trajectories of sun on summer and winter solstices are shown with two thin lines.

in Fig. 1. Figure 2 shows surrounding topography at the AWS, which was obtained from a digital elevation model (DEM) provided as ASTER products. Trajectories of the sun on summer and winter solstices show that direct solar radiation in the morning is shaded about 1 hour both in summer and winter. The valley where the AWS was located runs east and west, and mountains are located on the north and south. The mean elevation angle is roughly 13°, which corresponds to about 22% of the whole sky in solid angle.

Multipoint observations of air temperature and ground surface temperature were carried out from 29 September to 8 October in 2003. In addition to these components, relative humidity was measured from 1 October to 11 October in 2004. Single vinyl chloride pipes were used as radiation shields for air temperature measurements under natural draft conditions. An infrared thermometer was used for measuring surface temperature of debris on the Thorthormi Glacier (Fig. 1). Thermistor sensors which were covered with sand of 1 cm thickness were used for measuring ground surface temperatures at the other sites. Total precipitation was measured on the right-bank of Lugge Glacier (LG) at 4649 m a.s.l. and at a peak of 5043 m a.s.l. whose positions are shown in Fig. 1. Precipitation was measured from 29 September 2002 through 3 October 2003, and from 1 October 2002 through 8 October 2003, respectively. Brightness temperature images around glaciers were obtained using an infrared thermal imager (inframetrics MODEL 760). The accuracy of the temperature is ±2℃ and the minimum detectable temperature difference is within 0.2℃. Observed brightness temperature varies with air temperature and amount of precipitable water through a column between a target and the infrared thermal imager. Thus, the accuracy as well as spatial resolution depends on the distance to a given target. The images were taken in the daytime on only fine days October 1–11 October in 2004 to avoid the abovementioned problem, because the air is relatively dry and thin due to high altitudes. Descriptions of above multipoint observations are shown in Table 2.

3. Results and discussion

3.1 Lugge AWS

3.1.1 Temperatures

Figure 3a shows the seasonal variation of daily mean air temperature and ground surface temperature. They show typical sinusoidal-shape annual variations. The air temperatures ranged from −14℃ to 9℃. The annual mean air temperature was approximately 0℃, and the mean air temperature from the beginning of June to the end of September was 6℃. From the end of May to the beginning of October, the daily mean air temperature was higher than 0℃. As seen in the air temperature variations, dis-

Table 2. Description of observation points shown in Fig. 1. Air temperature (Ta), ground surface temperature (Ts) and relative humidity (Rh) were measured 2 m above ground. Differences in altitudes among AWS, TD and LO are less than 50 m.

Symbol	Description of site	Components	
		2003	2004
TD	Debris-covered area on Thorthormi Glacier		Ta, Ts, Rh
LO	Bare soil area around outlet of Lugge Glacier		Ta, Ts, Rh
5043 m	Grass area at 5043 m a.s.l.	Ta, Ts, P (Oct., 2002-)	Ta, Ts, Rh
LG	Right-bank of Lugge Glacier	P (Sep., 2002-)	
LGG	Water surface of Lugge Glacial Lake		Ts
IR1	Grass area near 5043 m		IR image (facing south)
IR2	Side moraine of Thorthormi Glacier		IR image (facing west)

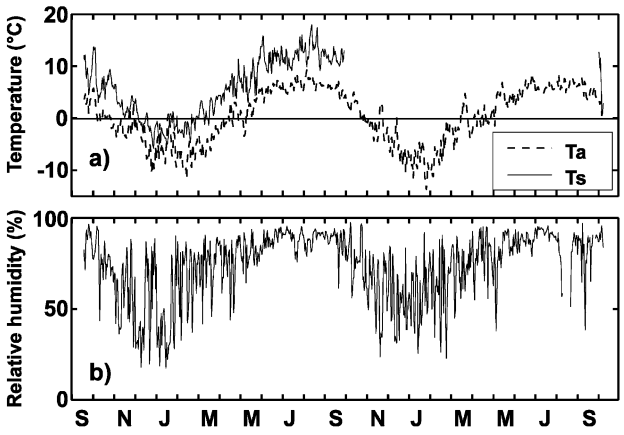

Fig. 3. Daily mean air temperature, ground temperature (a) and relative humidity (b) at Lugge AWS from 18 September, 2002 to 11 October, 2004.

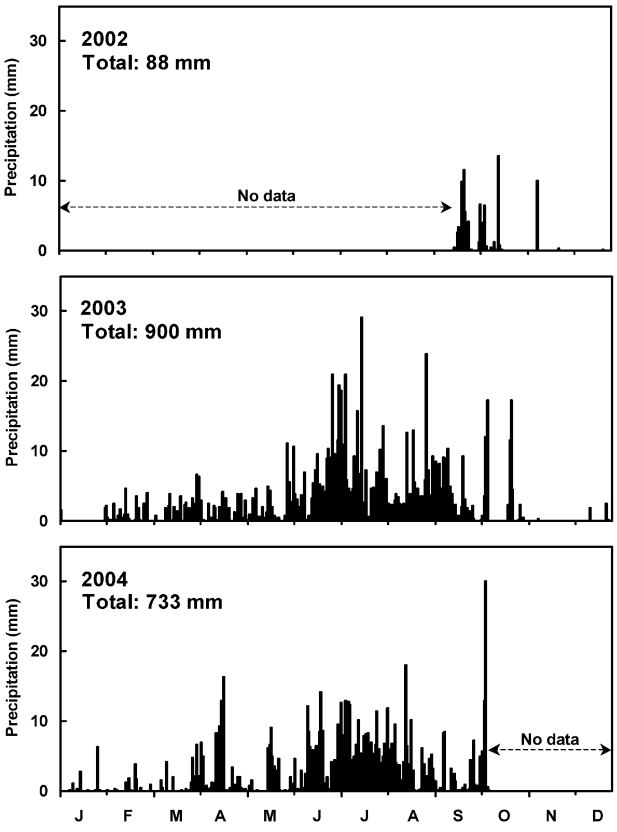

Fig. 4. Daily precipitation at Lugge AWS from 18 September to 31 December, 2002, January to December in 2003 and 1 January to 11 October, 2004. Totals through each observation period in each year are shown at upper left.

tinct seasonal variations were also found in the ground surface temperature, which was above 0℃ from March to October and ranged from −6℃ to 18℃.

3.1.2 Relative humidity

The daily mean relative humidity was higher and rather stable in summer, and lower and rather variable in winter (Fig. 3b). The relative humidity ranged from 20% to 95% throughout the year. The variability in relative humidity may be due to the frequency of precipitation. Mean relative humidity from June to September during the summer monsoon season was 89%, against 67% in other months.

3.1.3 Precipitation

Figure 4 shows daily precipitation from 18 September in 2002 to 10 October in 2004. The precipitation increases in summer monsoon season and decreases in winter. Over 70% of the total precipitation was observed from June to September in 2003. The amount of winter precipitation is uncertain due to undetected snowfall and freezing of the precipitation gauge.

Total precipitation for each observed period is also shown in Fig. 4. Naito *et al.* (2006) reported from observations in 1998–1999 (340 days) that the annual precipitation beside the Jichu Dramo Glacier, which is located at 5245 m a.s.l. 20 km south of Lugge AWS, was greater than 1349 mm. On the other hand, the annual precipitation was 900 mm in this region (Fig. 4b). Since the observed periods were different, it is difficult to explain these differences. However, these data imply spatial variability of precipitation.

3.1.4 Radiation

Daily mean downward shortwave radiation is shown in Fig. 5a. Differences between the observed and calculated values at the top of the atmosphere increase in summer due to cloud cover as suggested in

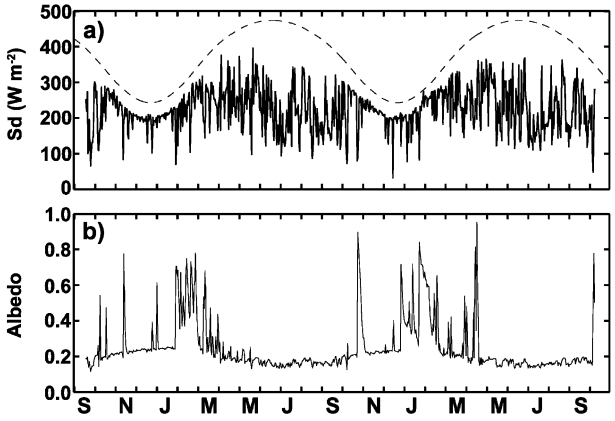

Fig. 5. Daily mean downward shortwave radiation (a) and albedo (b) at Lugge AWS from 18 September, 2002 to 11 October, 2004. Daily mean downward shortwave radiation at top of atmosphere (TOA) is also shown by dashed line in a).

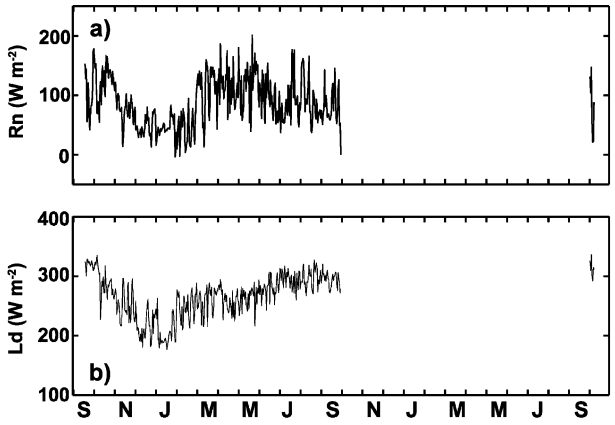

Fig. 6. Daily mean net radiation (a) at Lugge AWS and calculated downward longwave radiation (b) using observed net radiation, shortwave radiation and surface temperature at each time interval.

Fig. 4.

Albedo was calculated from the upward shortwave radiation divided by downward shortwave radiation (Table 1). Abnormal values above 1.0, which were considered to be due to snow accretion on the sensor, were eliminated from albedo. Figure 5b shows variations in daily mean albedo from 18 September 2002 to 10 October 2004. Increase of albedo in winter indicates the occurrence of snow cover at Lugge AWS in winter. Snow cover disappearance dates, when variation of ground temperatures were mild at around 0℃, increases from October 2002 to the following May. These data show that snowfall and melting of snow covers often occurred at the AWS in the winter.

Figure 6a shows daily mean values of net radiation. Downward radiation to the ground corresponds to a positive value. In winter, the net radiation is relatively small due to the increase of albedo (Fig. 5b). The data show net radiation in spring is relatively large independently of albedo. A similar seasonal variation to Fig. 5a was observed.

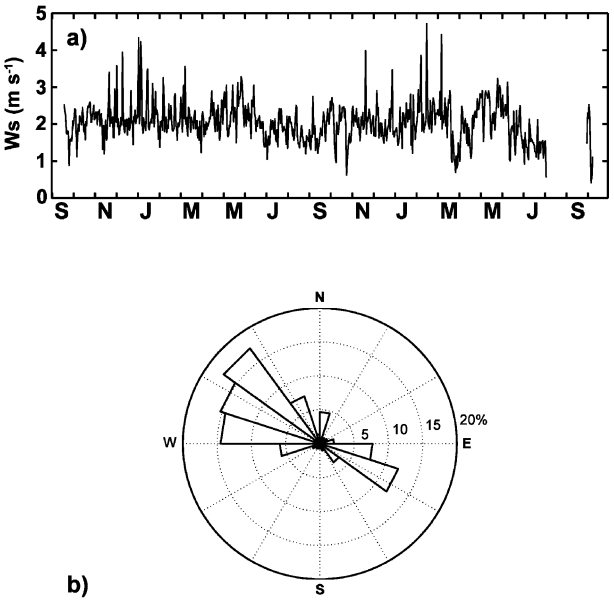

Fig. 7. Daily mean wind speeds (a) and histogram of wind directions (b) at Lugge AWS from 18 September, 2002 to 11 October, 2004. Total number of wind direction data is 36240.

Balance of shortwave radiation and upward longwave radiation were subtracted from the observed net radiation to obtain downward longwave radiation. The upward longwave radiation was calculated using the ground surface temperature shown in Fig. 3a, assuming that the ground can be regarded as a black body. Figure 6b shows daily mean downward longwave radation from 18 September in 2002 to 10 October in 2004. The mean downward longwave radiation from June through September 2003 was 291 W m^{-2}, while the mean downward shortwave radiation was 207 W m^{-2} for the same period. The data show that the downward longwave radiation decreases in winter and increases in summer. The cause of such variation is considered to be the seasonal variation of air temperature and cloud cover.

3.1.5 Wind speed and direction

Figure 7a shows daily mean wind speeds and Fig. 7b indicates the frequency distribution of wind directions calculated for every 18°. Relatively large wind speeds were observed in winter, but no definite seasonality was observed. About 70% of all observed data were concentrated in the east and west directions, which corresponds to the direction of the valley (Fig. 2). The data show that the air flows up and down along the valley. The diurnal cycle of wind speed in summer is presented in the following section.

3.1.6 Diurnal variations

Figure 8 shows monthly mean diurnal variations

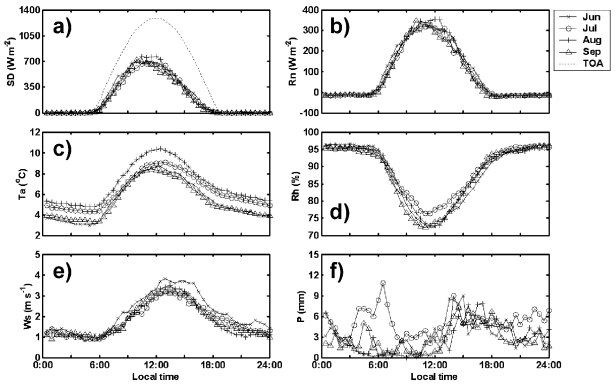

Fig. 8. Monthly mean diurnal variations of downward shortwave radiation (a), net radiation (b), air temperature (c), relative humidity (d) and wind speed (e) from June to September, 2003 and monthly precipitations (f) for each local time at Lugge AWS from June to September, 2003. Dashed line in Fig. 8a denotes downward shortwave radiation at top of atmosphere (TOA) averaged for June to September.

of downward shortwave radiation, net radiation, air temperature, relative humidity and wind speed from June to September in 2003. The monthly precipitation for each local time in the same period is plotted in Fig. 8f. All components show definite diurnal variations in association with solar insolation.

The observed shortwave radiation rapidly decreases in the afternoon compared to the value at the top of the atmosphere (Fig. 8a). This is not due to the effect of shading by surrounding mountains but rather to the attenuation of solar radiation by cloud cover in the afternoon which is caused by local circulation (Ageta, 1976), because the surrounding topography cannot shade the AWS from direct solar radiation during most of the daytime hours (Fig. 2). Figure 8b shows that the net radiation varies with the downward shortwave radiation, because the exchange of shortwave radiation controls the diurnal variation in net radiation (*e.g.,* Mattson and Gardner, 1991).

The variations in air temperature and relative humidity show an inverse relationship (Fig. 8c; Fig. 8 d). Figure 8e shows that relatively warm and dry wind increase in the daytime. The phases of wind speeds delay slightly compared to the other elements (Fig. 8e). Since the mountain and valley wind system is dominant in this region as shown in Fig. 7, the delay could be due to the time lag of heating between ground surface and atmosphere. However, no clear diurnal cycle of wind direction was recognized from June to September 2003. Figure 8f shows increases of precipitation from afternoon to early morning due to the local circulation. The same characteristic was also reported in previous studies (*e.g.,* Ageta, 1976; Ueno *et al.,* 2001).

3.2 Distribution of brightness temperature

Surface temperature is one of the key physical variables to investigate thermal property of a debris layer (Nakawo and Young, 1981; 1982). However, extensive measurement of surface temperature was not available on debris-covered glaciers due to the large size and heterogeneity of such glaciers. Brightness temperature, which can be obtained remotely using airborne and spaceborne thermal sensors (*e.g.,* Yasunari, 1980; Wessels *et al.,* 2002), also represents the energy amount on ground surfaces; while it is distinguished as a different physical variable from surface temperature (Kobayashi *et al.,* 2001).

Ground-based measurements of brightness temperature were carried out to investigate thermal environment around the glaciers in this region using a thermal infrared camera. Figure 9a is a pseudo color image of brightness temperature in the daytime on the terminal area of Thorthormi Glacier taken from the left side moraine, and Fig. 9b is a photograph of the corresponding area. The brightness temperature varies on the glacier in association with thickness and thermal properties of debris cover. The ice at the lower left of Fig. 9a was covered with thick debris, and the brightness temperature on the area was relatively high. Furthermore, the brightness temperature in this area ranged from 0℃ to 17℃ due to the presence of ice cliffs and warmed boulders of varied sizes (Fig. 9c; Fig. 9d). The brightness temperature image of Lugge and Thorthormi Glaciers shown in Fig. 10a is taken from a point near 5043 m a.s.l. Figure 10b shows the view around the corresponding area. Since the end moraine of Lugge Glacier is composed of relatively thick debris-covered ice as shown in Figs. 10c and 10d, the brightness temperature in this area is higher than on Thorthormi Glacier. As mentioned above, the thickness distribution of debris cover affects the surface temperature and could result in a complex ice melt pattern in this area (*e.g.,* Rana *et al.,* 1997; Nakawo *et al.,* 1999).

3.3 Multipoint observations

Table 3 shows a comparison of the total precipitation observed at three points around the glaciers (Fig. 1, Table 2). The precipitation at 5043 m was roughly nine- tenths of those at the other points. Ageta (1976) reported characteristic distribution of precipitation in the Nepal Himalayas due to the orographic effect on precipitation. Three observation points in this region were relatively close to each other, and the differences in observed precipitations are smaller than those reported in Ageta (1976).

Daily fluctuation of air temperature and ground surface temperature was compared using the data obtained at Lugge AWS and 5043 m a.s.l. in 2003. No time lags between the points were recognized in these data. The observed air temperatures at the AWS were 3.2℃ higher on average. The mean lapse rate of

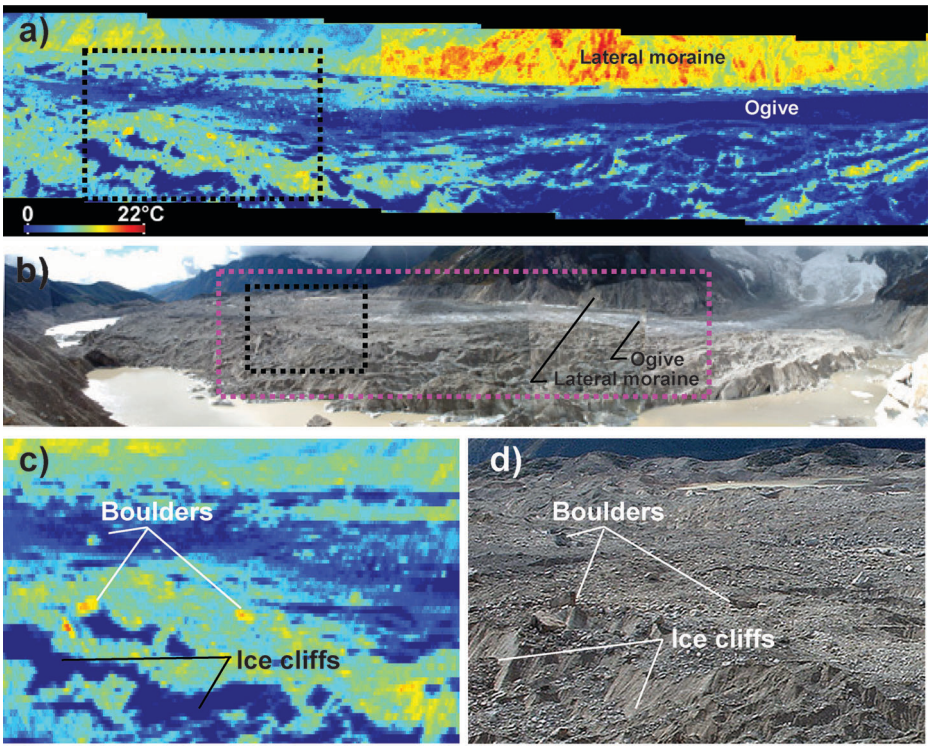

Fig. 9. a) Pseudo color image of brightness temperature on Thorthormi Glacier taken at 9: 30 on 5 October, 2004. b) Photo with corresponding view angle in Fig. 9a shown by violet dashed line. Black dashed lines in Figs. 9a and 9b denote corresponding view angle of close-up pictures shown in Figs. 9c and 9d, respectively.

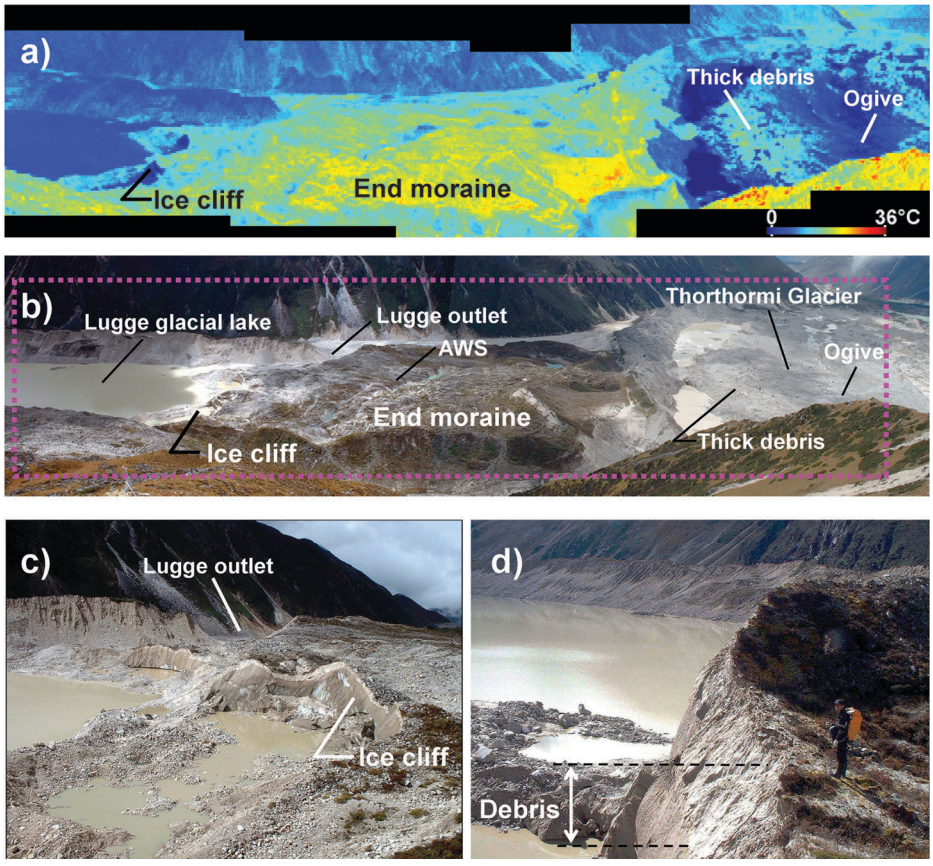

Fig. 10. a) Pseudo color image of brightness temperature around end moraine of Lugge Glacier (left) and Thorthormi Glacier (right) taken at 13:00 on 3 October, 2004. b) Photo with corresponding view angle of Fig. 10a shown by the violet dashed line. Photos c) and d) are ice cliffs at end moraine of Lugge Glacier.

Table 3. Comparison of total precipitations.

Point	Altitude (m a.s.l.)	Total precipitation (mm)	
		29 Sep., 2002 - 3 Oct., 2003	1 Oct., 2002 - 8 Oct., 2003
AWS	4524	868	869
LG	4649	928	-
5043 m	5043	-	825

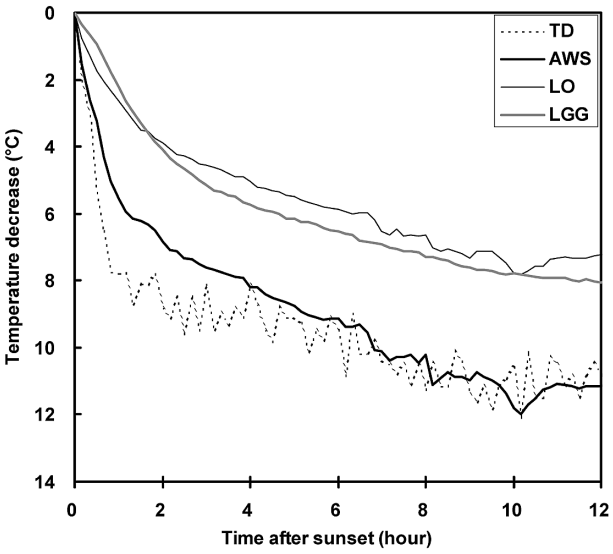

Fig. 11. Ground surface temperature decrease at 4 observation points (Fig. 1, Table 2) from sunset 2 October, 2004 until early the following morning.

air temperature in this period was 6.1℃ km^{-1}. On the other hand, the ground surface temperature at AWS averaged only 0.9℃ higher. Since differences in mean albedo at the two observation points were negligible, the energy absorbed through shortwave radiation, a dominant energy source of ground surfaces, was not a cause of the different surface temperatures. Figure 11 shows the temperature decrease on ground surface observed at 4 points (Fig. 1) from sunset on 2 October 2004 to early the following morning. The decrease of temperature at Thorthormi Glacier (TD) and Lugge AWS (AWS) was nearly 4℃ lower than at the other 2 points. The data need to be analyzed based on the heat balance method to identify the cause of this difference, but it implies a possibility of the presence of ice under the AWS because the amounts of decrease are considered to be due to different thermal properties among the observation points (Kondo, 2000).

The data obtained from the multipoint observations in 2004 (Table 2) about air temperature, ground surface temperature and relative humidity were compared. A lapse rate of air temperature observed between Lugge AWS and 5043 m a.s.l. in this period resulted in 5.4℃ km^{-1}, which is smaller than that obtained in 2003. The cause of this difference is not clear, but the bad weather conditions in the beginning of October in 2004 may be related. The mean of above lapse rates is approximately 6℃ km^{-1}, which is the same value reported by Naito *et al.* (2006) around Jichu Dramo Glacier in Bhutan.

The ground surface temperatures observed at 4 points (Table 2, Fig. 1) were affected by snow cover during the observed period. The weather was fair in the first half and snowy in the last half of the period. The maximum difference among the temperatures observed at 4 points averaged 8℃. In the first half, the differences decreased in the daytime and increased in the nighttime. This characteristic was explained by the rapid temperature decrease at Thorthormi Glacier after sunset, and is considered to be due to the relatively thin debris layer on ice. As shown in Fig. 11, ground surface temperatures on debris-covered ice decreased rapidly and largely compared to those on other surfaces. Similar results were obtained in previous studies, which observed higher air temperature in the debris-covered area than in the debris-free area due to the effect of heat storage of debris (*e.g.,* Fujita and Sakai, 2000; Takeuchi *et al.,* 2000).

The relative humidity observed at 5043 m a.s.l. showed saturated condition during the observation period. On the other hand, no clear difference in relative humidity was observed among the other points. The data ranged from 36% to 98%, and it varied inversely with air temperature and ground surface temperature as shown in Fig. 8d.

4. Summary

Investigations of meteorological conditions around debris-covered glaciers and glacial lakes in the Lunana region of Bhutan were carried out from September, 2002 to October, 2004. The characteristics of variations and average values of each meteorological element were shown using the data observed by Lugge AWS. The data observed at different sites indicated that spatial variability of surface temperatures was relatively large compared to the air temperature and relative humidity. These data will be helpful for mass balance and glacial lake studies in this region.

Acknowledgments

We would like to express thanks to everyone who so generously cooperated in obtaining data from the

field observations. In particular, we are grateful to the Geological Survey of Bhutan and Dr. Akiko Sakai of Nagoya University. The manuscript was much improved by useful comments from Dr. Takeshi Yamazaki and Dr. Keiko Konya. The copyright for ASTER data is reserved by the Ministry of Economy, Trade and Industry of the Japanese Government. This study was supported by the Announcement of Research Opportunity (ASTER ARO, AP-0006) and a Grant-in-Aid for Scientific Research (Project: 13373006; 13573004; G-4, the 21st Century COE Program) from the Ministry of Education, Culture, Sports, Science and Technology of Japan.

References

Ageta, Y. (1976): Characteristics of precipitation during monsoon season in Khumbu Himal. Seppyo, **38**, Special issue, 84–88.

Ageta, Y., Iwata, S., Yabuki, H., Naito, N., Sakai, A., Narama, C. and Karma (2000): Expansion of glacier lakes in recent decades in the Bhutan Himalayas. *In* Nakawo, M., Raymond, C.F. and Fountain, A. (eds.), Debris-Covered Glaciers. IAHS Publ., **264**, 165–175.

Benn, D.I. and Lehmkuhl, F. (2000): Mass balance and equilibrium-line altitudes of glaciers in high-mountain environments. Quatern. Int., **65/66**, 15–29.

Fujii, Y. (1977): Field experiment on glacier ablation under a layer of debris cover. Seppyo, **39**, Special issue, 20–21.

Fujita, K. and Sakai, A. (2000): Air temperature environment on the debris-covered area of Lirung Glacier, Langtang Valley, Nepal Himalayas. *In* Nakawo, M., Raymond, C.F. and Fountain, A. (eds.), Debris-Covered Glaciers. IAHS Publ., **264**, 83–88.

Iwata, S., Ageta, Y., Naito, N., Sakai, A., Narama, C. and Karma (2002): Glacier lakes and their outburst flood assessment in the Bhutan Himalaya. Global Environ. Res., **6**, 3–17.

Kobayashi, T., Tani, H., Kurose, Y., Tsukamoto, O., Igarashi, T., Kashiwagi, Y., Kuwagata, T., Toritani, H., Mori, M. and Wakimizu, K. (2001): For good use of infrared thermometers and infrared thermal imagers in local meteorology (in Japanese). J. Agric. Meteorol., **57**, 107–115.

Komori, J., Gurung, D.R., Iwata, S. and Yabuki, H. (2004): Variation and lake expansion of Chubda Glacier, Bhutan Himalayas, during the last 35 years. Bull. Glaciol. Res., **21**, 49–55.

Kondo, J. (2000): Atmospheric science near the ground surface (in Japanese). University of Tokyo Press, 324 pp.

Mattson, L.E. and Gardner, J.S. (1991): Energy exchanges and ablation rates on the debris-covered Rakhiot Glacier, Pakistan. Zeitschrift Für Gletscherkunde Und Glazialgeolgie, **25**, 17–32.

Mattson, L.E., Gardner, J.S. and Young, G.J. (1993): Ablation on debris covered glaciers: an example from the Rakhiot Glacier, Punjab, Himalaya. *In* Young, G.J. (ed.), Snow and Glacier Hydrology, IAHS Publ., **218**, 289–296.

Naito, N., Ageta, Y., Iwata, S., Matsuda, Y., Suzuki, R., Karma and Yabuki, H. (2006): Glacier shrinkages and climate conditions around Jichu Dramo Glacier in the Bhutan Himalayas from 1998 to 2003. Bull. Glaciol. Res., **23**, 51–61.

Nakawo, M. and Young, G.J. (1981): Field experiments to determine the effect of a debris layer on ablation of glacier ice. Ann. Glaciol., **2**, 85–91.

Nakawo, M. and Young, G.J. (1982): Estimate of glacier ablation under a debris layer from surface temperature and meteorological variables. J. Glaciol., **28**, 29–34.

Nakawo, M. and Rana, B. (1999): Estimate of ablation rate of glacier ice under a supraglacial debris layer. Geografiska Annaler, **81A**, 695–701.

Rana, B., Nakawo, M., Fukushima, Y. and Ageta, Y. (1997): Application of a conceptual precipitation-runoff model (HYCYMODEL) in a debris-covered glacierized basin in the Langtang Valley, Nepal Himalaya. Ann. Glaciol., **25**, 226–231.

Richardson, S.D. and Reynolds, J.M. (2000): An overview of glacial hazards in the Himalayas. Quatern. Int., **65/66**, 31–47.

Takeuchi, Y., Kayastha, R.B. and Nakawo, M. (2000): Characteristics of ablation and heat balance in debris-free and debris-covered areas on Khumbu Glacier, Nepal Himalayas, in the pre-monsoon season. *In* Nakawo, M., Raymond, C.F. and Fountain, A. (eds.), Debris-Covered Glaciers. IAHS Publ., **264**, 53–61.

Ueno, K., Kayastha, R.B., Chitrakar, M.R., Bajracharya, O.R., Pokhrel, A.P., Fujinami, H., Kadota, T., Iida, H., Manandhar, D.P., Hattori, M., Yasunari, T. and Nakawo, M. (2001): Meteorological observations during 1994–2000 at the Automatic Weather Station (GEN-AWS) in Khumbu region, Nepal Himalayas. Bull. Glaciol. Res., **18**, 23–30.

Wessels, R.L., Kargel, J.S. and Kieffer, H.H. (2002): ASTER measurement of supraglacial lakes in the Mount Everest region of the Himalaya, Ann. Glaciol., **34**, 399–408.

Yamada, T., Naito, N., Kohshima, S., Fushimi, H., Nakazawa, F., Segawa, T., Uetake, J., Suzuki, R., Sato, N., Karma, Chhetri, I.K., Gyenden, L., Yabuki, H. and Chikita, K. (2004): Outline of 2002 — research activities on glaciers and glacier lakes in Lunana region, Bhutan Himalayas. Bull. Glaciol. Res., **21**, 79–90.

Yasunari, T. (1980): Air-borne measurements of the surface temperature over the Nepal Himalayas. Seppyo, **42**, Special issue, 82–85.